Hindawi
Discrete Dynamics in Nature and Society
Volume 2020, Article ID 6048438, 8 pages
https://doi.org/10.1155/2020/6048438

Research Article

On Face Index of Silicon Carbides

Xiujun Zhang,[1] **Ali Raza**,[2] **Asfand Fahad**,[2] **Muhammad Kamran Jamil**,[3] **Muhammad Anwar Chaudhry**,[4] **and Zahid Iqbal**[4,5]

[1]*School of Information Science and Engineering, Chengdu University, Chengdu 610106, China*
[2]*Department of Mathematics, COMSATS University Islamabad, Vehari Campus, Vehari 61110, Pakistan*
[3]*Department of Mathematics, Riphah Institute of Computing and Applied Sciences, Riphah International University, 14 Ali Road, Lahore, Pakistan*
[4]*Department of Mathematics and Statistics, Institute of Southern Punjab, Multan 66000, Pakistan*
[5]*School of Natural Sciences, National University of Sciences and Technology, Sector H-12, Islamabad, Pakistan*

Correspondence should be addressed to Muhammad Kamran Jamil; m.kamran.sms@gmail.com

Received 13 May 2020; Accepted 4 July 2020; Published 1 August 2020

Academic Editor: Juan L. G. Guirao

Several graph invariants have been defined and studied, which present applications in nanochemistry, computer networks, and other areas of science. One vastly studied class of the graph invariants is the class of the topological indices, which helps in the studies of chemical, biological, and physical properties of a chemical structure. One recently introduced graph invariant is the face index, which can assist in predicting the energy and the boiling points of the certain chemical structures. In this paper, we drive the analytical closed formulas of face index of silicon carbides $Si_2C_3 - \mathrm{I}[a,b]$, $Si_2C_3 - \mathrm{II}[a,b]$, $Si_2C_3 - \mathrm{III}[a,b]$, and $SiC_3 - \mathrm{III}[a,b]$.

1. Introduction

Several invariants assigning a matrix, a polynomial, a numeric number, or a sequence (of numbers) to a graph have been defined and studied during the last few decades. One such significant class among such invariants is the class of topological indices (TIs), which assigns a number to the given graph. The value of a TI of a molecular structure is dependent on its shape, size, symmetry, patterns of the bonds, and the contents of heteroatoms in it. Consequently, the notion of the TI provides the quantitative characterization of the molecular structures. Several researchers have studied different aspects and applications of the TIs. For contents related to studies on lower/upper bounds maxima/minima of TIs, see [1–5], studies on chemistry and drugs see [6–10], and other applications, see [11–13]. Another vital contribution of the study of the TIs is their effectiveness in studying the different aspects of new drugs and chemical compounds, which is an immense need of the medical science and industry. For details, we refer [14, 15] to the readers. Consequently, computing and studying the behavior of the values of the TIs of the molecular structures provide significant information and hence is one of the trends in modern research.

Before proceeding further with the study of a specific index, we set the notations used in this paper. The notions of a planar graph, its faces, and an infinite face are well known in the literature. Let G be a graph with vertex set $V(G)$, edge set $E(G)$, and face set $F(G)$. A face f is said to be incident with an edge e, whenever e is among the edges which surrounds f. Moreover, face is said to be incident with a vertex w, whenever w is incident to an edge e which surrounds f. The incidency of w to the face f is represented by $w \sim f$. The degree of a face f in G is given as $d(f) = \sum_{w \sim f} d_w$. For the notions and notations not given here, we refer [16] to the readers. Recently, Jamil et al. [17] introduced a novel topological index named as the face index. They showed that the face index can help to predict the boiling points and the energy of selected benzenoid hydrocarbons with the correlation coefficient $r > 0.99$. For a planar graph G, the face index (FI) can be defined as

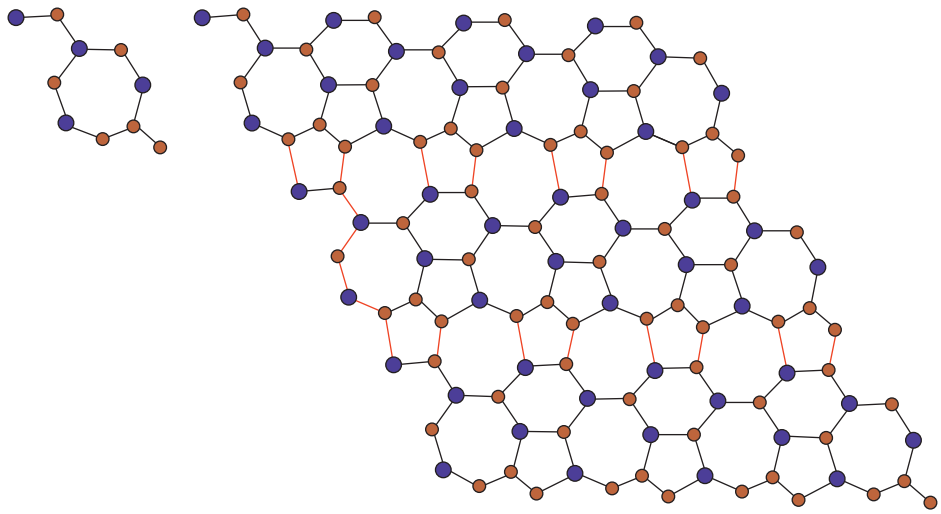

(a) (b)

Figure 1: The unit cell and $Si_2C_3 - I[3,4]$, respectively.

$$\mathrm{FI}(G) = \sum_{f \in F(G)} d(f) = \sum_{w \sim f \in F(G)} d_w, \tag{1}$$

where $w \sim f$ represents the incidency of the vertex w with the face f.

On the contrary, the Silicon Carbide (SiC) is the first and foremost material that contained the covalent bound of C and Si atoms, typically in biatomic layers. These layers form tetrahedrally oriented molecules of C and Si atoms, with a very short bound length and hence a very high bound strength. This is the base of extremely high mechanically and chemical stability of SiC [18, 19]. SiC occurs in nature as the incredibly uncommon mineral moissanite. SiC being one of the most extensively used wide bandgap materials, performs a vital role in power industries by setting new principles in power savings as rectifiers or switches in the system for data centers, solar cells, wind turbines, and electric vehicles, as well as high temperature and radiation tolerant electronic applications [20–23]. There are several silicon carbides which we are going to study in this paper, such as $Si_2C_3 - I[a,b]$, $Si_2C_3 - II[a,b]$, $Si_2C_3 - III[a,b]$, and $SiC_3 - III[a,b]$. Several papers have been devoted to the study of silicon, carbon-based structures, for details, see [24–26]. The main objective of this paper is to find the analytic formula of the face index of these silicon carbides. Moreover, we also present the graphical analysis of the obtained results. For this, we use the Chemsketch for plotting the figures of silicon carbides, Maple for calculations, and MATLAB for graphical analysis.

Before presenting the results, we include Euler's formula for planar graphs. Evidently, we may observe that the silicon structures presented in Section 2 are consistent with this formula.

Theorem 1. *For a finite, connected, and planar graph G with vertex set $V(G)$, edge set $E(G)$, and face set $F(G)$, we have*

$$|V(G)| - |E(G)| + |F(G)| = 2. \tag{2}$$

2. Results

In this section, we investigate the exact formulas of the face index for $Si_2C_3 - I[a,b]$, $Si_2C_3 - II[a,b]$, $Si_2C_3 - III[a,b]$, and $SiC_3 - III[a,b]$. To find the face indices of the molecular graphs, we partitioned the face set depending on the degrees of each face.

2.1. Face Index for $Si_2C_3 - II[a,b]$ and Graphical Representations. The molecular graphs of silicon carbides $Si_2C_3 - I[a,b]$ are given in Figure 1. Figure 1(a) consists of unit cell of the silicon carbide $Si_2C_3 - I[a,b]$ and $Si_2C_3 - I[a,b]$ for $a = 1$ and $b = 1$. Figure 1(b) is $Si_2C_3 - I[a,b]$ for $a = 3$ and $b = 4$.

Theorem 2. *Let $G = Si_2C_3 - I[a,b]$, where $a, b \geq 1$. Then,*

$$\mathrm{FI}(G) = \begin{cases} 70a - 34, & \text{if } b = 1 \\ 90ab - 20a - 30b - 4, & \text{if } a, b \neq 1 \\ 18(3b - 1), & \text{if } a = 1. \end{cases} \tag{3}$$

Proof. We consider the following three cases:

Case-I If $b = 1$, let f_j and $|f_j|$ denote the face with the property $\sum_{w \sim f_j} d_w = j$ and the number of such faces, respectively. The structure $Si_2C_3 - I[a,1]$ contains four types of internal faces f_{14}, f_{16}, f_{18}, and f_{20} and an external face, f_∞. So, the face index of Si_2C_3-$I[a,1]$ is

Table 1: Numbers of f_{14}, f_{15}, f_{16}, f_{18}, f_{19}, f_{20}, and f_{21} with given number of rows.

Rows	$\lvert f_{14}\rvert$	$\lvert f_{15}\rvert$	$\lvert f_{16}\rvert$	$\lvert f_{18}\rvert$	$\lvert f_{19}\rvert$	$\lvert f_{20}\rvert$	$\lvert f_{21}\rvert$
2	a + 1	2a−3	a−1	a + 1	2	a−2	2a−3
3	a + 3	2(2a−3)	a−1	2a	4	a−2	2(2a−3)
4	a + 5	3(2a−3)	a−1	3a−1	6	a−2	3(2a−3)
.	.	.	.	.	—	—	—
.	.	.	.	.	—	—	—
.	.	.	.	.	—	—	—
B	a + 2b−3	(b−1) (2a−3)	a−1	ab−a−b + 3	2(b−1)	a−2	(b−1) (2a−3)

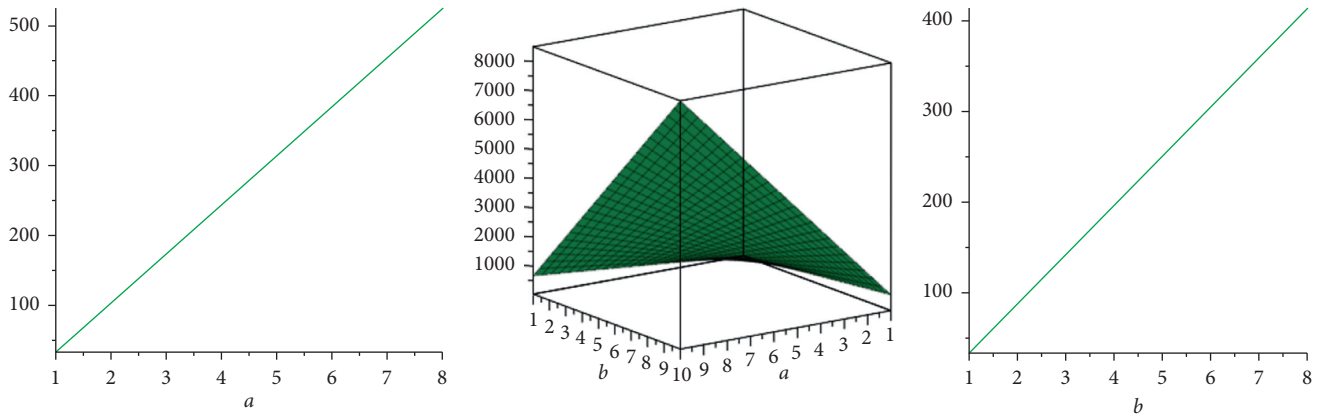

(a) (b) (c)

Figure 2: FI$(Si_2C_3 - I[a, 1])$, FI$(Si_2C_3 - I[a, b])$, and FI$(Si_2C_3 - I[1, b])$, respectively.

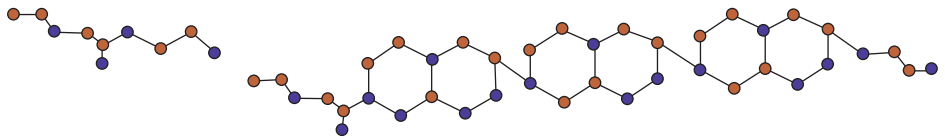

(a) (b)

Figure 3: The unit cell and $Si_2C_3 - II[4, 1]$, respectively.

$$\begin{aligned} FI(G) &= \sum_{w \sim f \in F(G)} d_w \\ &= \sum_{w \sim f_{14}} d_w + \sum_{w \sim f_{16}} d_w + \sum_{w \sim f_{18}} d_w + \sum_{w \sim f_{20}} d_w + \sum_{w \sim f_{\infty}} d_w \\ &= |f_{14}|(14) + |f_{16}|(16) + |f_{18}|(18) + |f_{20}|(20) + 20a \\ &= 14(a-1) + 16(a-1) + 18(2) + 20(a-2) + 20a \\ &= 70a - 34. \end{aligned} \tag{4}$$

Case-II When $a, b \neq 1$, then, we notice that the structure $Si_2C_3 - I[a, b]$ contains seven types of faces, which are f_{14}, f_{15}, f_{16}, f_{18}, f_{19}, f_{20}, and f_{21} and an external face, f_{∞}. Moreover, the sum of vertex degrees of external face is $20a + 30(b - 1)$. In each row of Table 1, the number of internal faces is written.

Table 2: Numbers of f_{16}, f_{17}, and f_{18} with given number of rows.

No. of rows	$\lvert f_{16}\rvert$	$\lvert f_{17}\rvert$	$\lvert f_{18}\rvert$
2	2a	2a	3a−5
3	2a + 2	2a + 2	8a−12
4	2a + 4	2a + 4	13a−19
.	.	.	.
.	.	.	.
.	.	.	.
B	2(a + b)−4	2(a + b)−4	5ab−7(a + b) + 9

The rest follows from the definition of the face index.

The face index of $Si_2C_3 - I[a, b]$ is

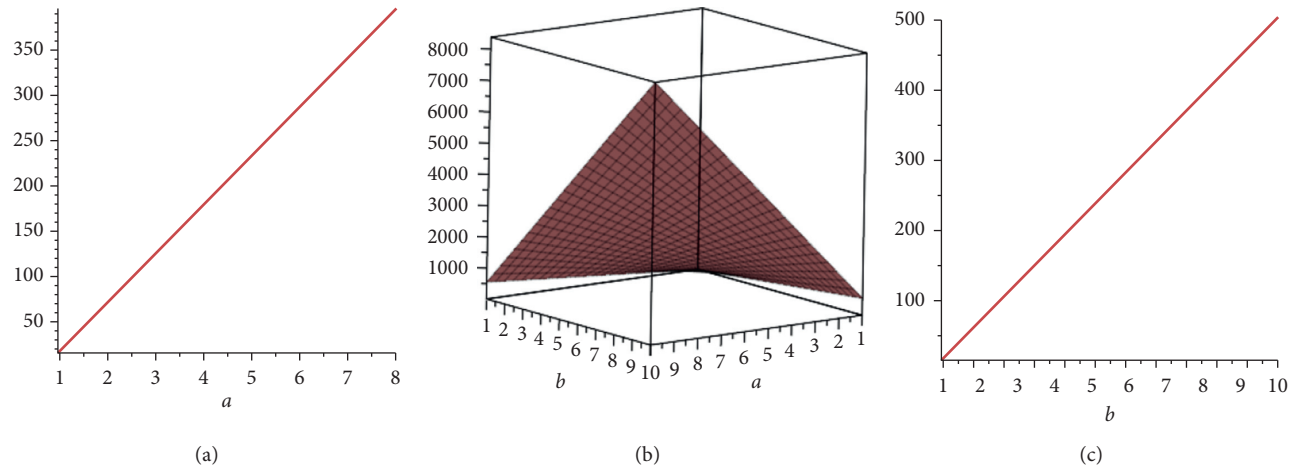

(a) (b) (c)

FIGURE 4: $\mathrm{FI}(Si_2C_3 - \mathrm{II}[a,1])$, $\mathrm{FI}(Si_2C_3 - \mathrm{II}[a,b])$, and $\mathrm{FI}(Si_2C_3 - \mathrm{II}[1,b])$, respectively.

$$\begin{aligned}
\mathrm{FI}(G) &= \sum_{w\sim f\in F(G)} d_w \\
&= \sum_{w\sim f_{14}} d_w + \sum_{w\sim f_{15}} d_w + \sum_{w\sim f_{16}} d_w + \sum_{w\sim f_{18}} d_w \\
&\quad + \sum_{w\sim f_{19}} d_w + \sum_{w\sim f_{20}} d_w + \sum_{w\sim f_{21}} d_w + \sum_{w\sim f_{\infty}} d_w \\
&= |f_{14}|(14) + |f_{15}|(15) + |f_{16}|(16) + |f_{18}|(18) \\
&\quad + |f_{19}|(19) + |f_{20}|(20) + |f_{21}|(21) + 20a + 30(b-1) \\
&= 14(a+2b-3) + 15(b-1)(2a-3) + 16(a-1) \\
&\quad + 18(ab-a-b+3) + 19(2(b-1)) + 20(a-2) \\
&\quad + 21(b-1)(2a-3) + 20a + 30(b-1) \\
&= 90ab - 20a - 30b - 4.
\end{aligned} \tag{5}$$

Case-III When $a = 1$, the structure $Si_2C_3 - \mathrm{I}[a,b]$ contains three types of internal faces f_{13}, f_{16}, and f_{17} and an external face f_∞ with sum of degrees $24b - 4$. Moreover, $|f_{13}| = b - 1$, $|f_{16}| = 1$, and $|f_{17}| = b - 1$. So, the face index of $Si_2C_3 - \mathrm{I}[a,b]$ is

$$\begin{aligned}
\mathrm{FI}(G) &= \sum_{w\sim f\in F(G)} d_w \\
&= \sum_{w\sim f_{13}} d_w + \sum_{w\sim f_{16}} d_w + \sum_{w\sim f_{17}} d_w + \sum_{w\sim f_{\infty}} d_w \\
&= |f_{13}|(13) + |f_{16}|(16) + |f_{17}|(17) + 24b - 4 \\
&= 13(b-1) + 16(1) + 17(b-1) + 24b - 4 \\
&= 18(3b-1),
\end{aligned} \tag{6}$$

which completes the proof. □

Remark 1. It is interesting to observe that $|V(Si_2C_3 - \mathrm{I}[a,b])| = 10ab$, $|E(Si_2C_3 - \mathrm{I}[a,b])| = 15ab - 2a - 3b$, and $|F(Si_2C_3 - \mathrm{I}[a,b])| = 5ab - 2a - 3b + 2$. Hence, the structure $Si_2C_3 - \mathrm{I}[a,b]$ satisfies the Euler formula.

Now, we present the results obtained for $Si_2C_3 - \mathrm{I}[a,b]$ in a graphical way in Figure 2. Every silicon carbide structure depends on two variables a and b. We use two kinds of graphs to show the outcomes of face index. One is the 2D graph where the reliance of a face index is drawn against one variable of the structure a or b while other is kept fixed. Here, we demonstrate 2D graphs for $b = 1$ and change a, and for $a = 1$ and change b. The second tool is the 3D graph where reliance of a face index is drawn against both parameters, and we gained a surface that tells about the trends of face index against both parameters a and b at the same time.

2.2. Face Index for $Si_2C_3 - II[a,b]$ and Graphical Representations. The molecular graphs of silicon carbides $Si_2C_3 - \mathrm{II}[a,b]$ are given in Figure 3, which consists of unit cell of silicon carbide $Si_2C_3 - \mathrm{II}[a,b]$ and $Si_2C_3 - \mathrm{II}[a,b]$ for $a = 4$ and $b = 1$.

Theorem 3. *Let $H = Si_2C_3 - II[a,b]$, where $a,b \geq 1$. Then, the face index of H is given as*

$$\mathrm{FI}(H) = \begin{cases} 18(3a-2), & \text{if } b = 1, \\ 90ab - 30(a+b) - 15, & \text{if } a,b \neq 1, \\ 18(3b-2), & \text{if } a = 1. \end{cases} \tag{7}$$

Proof. We consider the following three cases.

Case-I If $b = 1$, then the graph of $Si_2C_3 - \mathrm{II}[a,1]$ consists of two faces, an internal face f_{15} with $|f_{15}| = 2a - 2$ and an external face, f_∞ having the sum of vertex degrees $24a - 6$. The rest follows from the definition of the face index.

Case-II When $a,b \neq 1$, then, we notice that the structure $Si_2C_3 - \mathrm{II}[a,b]$ contains three types of internal faces, which are f_{16}, f_{17}, and f_{18} and an external face, f_∞. Moreover, the sum of vertex degrees of external face is $30(a+b) - 45$. The number of internal faces in each row is given in Table 2. □

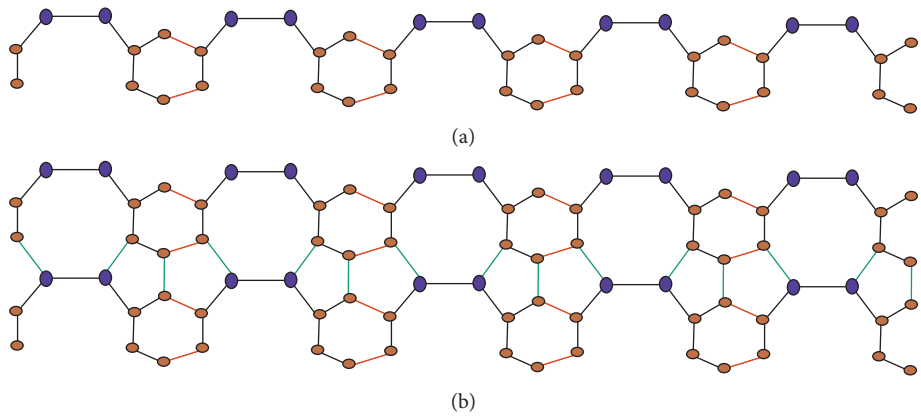

Figure 5: (a) $SiC_3 - \mathrm{III}[5,1]$ and (b) $SiC_3 - \mathrm{III}[5,2]$.

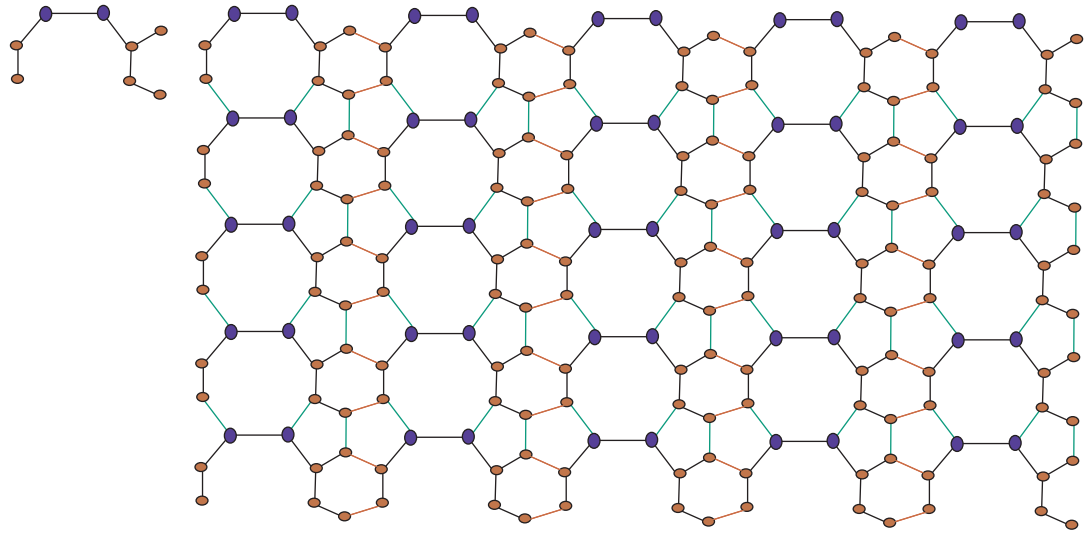

Figure 6: The unit cell and $SiC_3 - \mathrm{III}[5,5]$, respectively.

Case-III When $a = 1$, the structure $Si_2C_3 - \mathrm{II}[a,b]$ contains an internal face f_{15} and an external face f_∞ with sum of degrees $24b - 6$. Moreover, $|f_{15}| = 2b - 2$. The rest follows from the definition of the face index.

Remark 2. It is interesting to observe that $|V(Si_2C_3 - \mathrm{II}[a,b])| = 10ab$, $|E(Si_2C_3 - \mathrm{II}[a,b])| = 15ab - 2a - 3b$, and $|F(Si_2C_3 - \mathrm{II}[a,b])| = 5ab - 2a - 3b + 2$. Hence, the structure $Si_2C_3 - \mathrm{II}[a,b]$ satisfies the Euler formula.

With the same settings as in Section 2.1, we present the results obtained for $Si_2C_3 - \mathrm{II}[a,b]$ in graphical way in Figure 4.

2.3. Face Index for $SiC_3 - III[a,b]$ and Graphical Representations. The molecular graphs of silicon carbides $SiC_3 - \mathrm{III}[a,b]$ are given in Figures 5 and 6. Figure 5(a) is for $a = 5$ and $b = 1$, Figure 5(b) is for $a = 5$ and $b = 2$, and Figure 6 consists of unit cell and $SiC_3 - \mathrm{III}[a,b]$ for $a = 5$ and $b = 5$.

Table 3: Numbers of f_{13}, f_{15}, f_{17}, f_{18}, f_{20}, f_{22}, and f_{24} with given number of rows.

Rows	$\lvert f_{13}\rvert$	$\lvert f_{15}\rvert$	$\lvert f_{17}\rvert$	$\lvert f_{18}\rvert$	$\lvert f_{20}\rvert$	$\lvert f_{22}\rvert$	$\lvert f_{24}\rvert$
2	1	3(a−1)	a−1	—	1	a−1	—
3	2	5(a−1)	a−1	a−1	1	A	a−1
4	3	7(a−1)	a−1	2(a−1)	1	a + 1	2(a−1)
·	·	·	·	·	·	·	·
·	·	·	·	·	·	·	·
·	·	·	·	·	·	·	·
B	b−1	(2b−1) (a−1)	a−1	(b−2) (a−1)	1	a + b−3	(b−2) (a−1)

The rest follows from the definition of the face index.

Theorem 4. *Let $K = SiC_3 - III[a,b]$, where $a, b \geq 1$. Then,*

$$\mathrm{FI}(K) = \begin{cases} 32a - 18; & \text{for } b = 1 \\ 72ab - 30a - 20b - 7; & \text{for } b > 1. \end{cases} \quad (8)$$

Proof. When $b = 1$, then the graph of $SiC_3 - \mathrm{III}[a,1]$ consists of two faces, an internal face f_{14} with $|f_{14}| = a - 1$, and

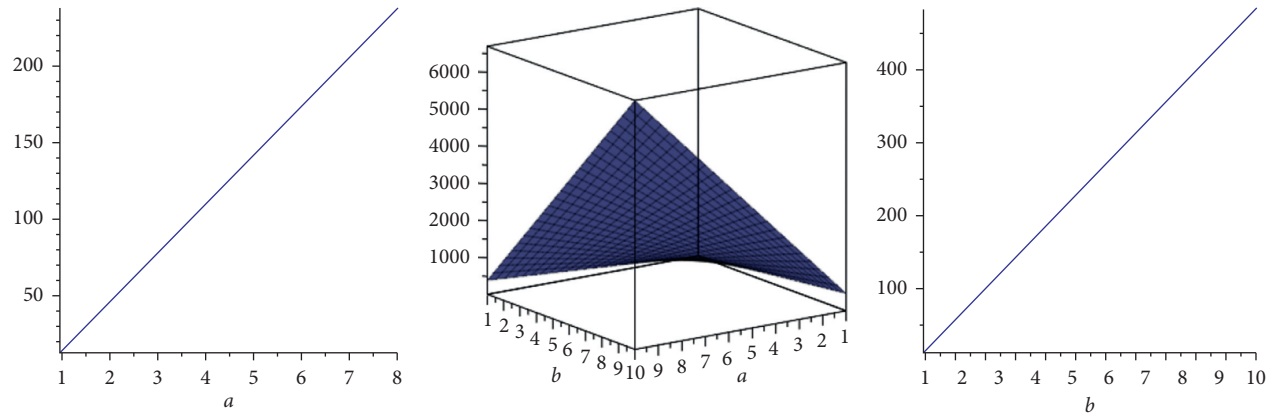

(a) (b) (c)

Figure 7: FI$(SiC_3 - \mathrm{III}[a,1])$, FI$(SiC_3 - \mathrm{III}[a,b])$, and FI$(SiC_3 - \mathrm{III}[1,b])$, respectively.

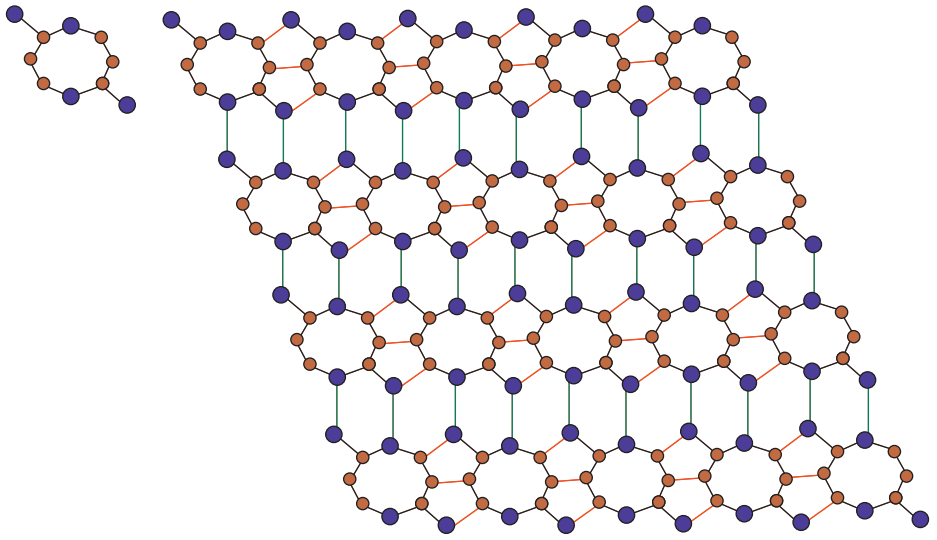

(a) (b)

Figure 8: The unit cell and $SiC_3 - \mathrm{III}[5,4]$, respectively.

an external face, f_∞ having the sum of degrees $18a - 4$. The rest follows from the definition of the face index. Now, when $b > 1$, then we notice that the structure $SiC_3 - \mathrm{III}[a,b]$ contains seven types of internal faces which are f_{13}, f_{15}, f_{17}, f_{18}, f_{20}, f_{22}, and f_{24} and an external face, f_∞. Moreover, the sum of vertex degrees of external face is $30a + 17b - 30$. In each row of Table 3, the number of internal faces is written. □

Remark 3. It is interesting to observe that $|V(SiC_3 - \mathrm{III}[a,b])| = 8ab$, $|E(SiC_3 - \mathrm{III}[a,b])| = 12ab - 3a - 2b$, and $|F(SiC_3 - \mathrm{III}[a,b])| = 4ab - 3a - 2b + 2$. Hence, the structure $SiC_3 - \mathrm{III}[a,b]$ satisfies the Euler formula.

With the same settings as in Section 2.1, we present the results obtained for $SiC_3 - \mathrm{III}[a,b]$ in a graphical way in Figure 7.

2.4. Face Index for $SiC_3 - III[a,b]$ and Graphical Representations. The molecular graphs of silicon carbides $SiC_3 - \mathrm{III}[a,b]$ are given in Figure 8.

Theorem 5. *Let $L = SiC_3 - III[a,b]$, where $a, b \geq 1$. Then,*

$$\mathrm{FI}(L) = \begin{cases} 70a - 32, & \text{for } b = 1, \\ 90ab - 20a - 30b - 2, & \text{for } b > 1. \end{cases} \quad (9)$$

Table 4: Numbers of f_{14}, f_{15}, f_{17}, f_{18}, f_{21}, f_{22}, f_{23}, and f_{24} with given number of rows.

No. of rows	$\|f_{14}\|$	$\|f_{15}\|$	$\|f_{17}\|$	$\|f_{18}\|$	$\|f_{21}\|$	$\|f_{22}\|$	$\|f_{23}\|$	$\|f_{24}\|$
2	2(a−1)	2(a−1)	2	(2a−3)	4	—	2(a−2)	—
3	2(a−1)	4(a−1)	4	2(2a−3)	4	2	2(a−2)	a−2
4	2(a−1)	6(a−1)	6	3(2a−3)	4	4	2(a−2)	2(a−2)
.	.	.	.	.	.	.	.	
.	.	.	.	.	.	.	.	
.	.	.	.	.	.	.	.	
B	2(a−1)	2(b−1) (a−1)	2(b−1)	(b−1) (2a−3)	4	2(b−2)	2(a−2)	(b−2) (a−2)

The rest follows from the definition of the face index.

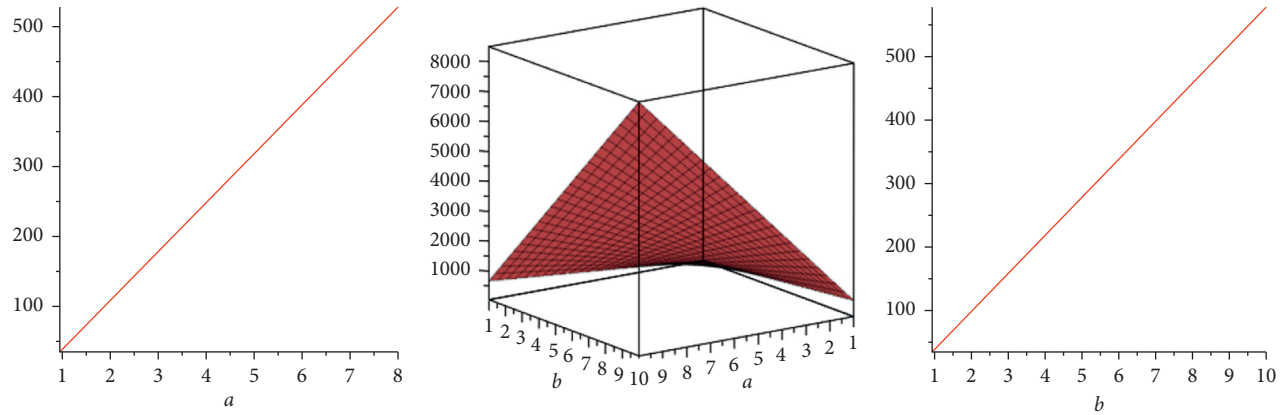

(a) (b) (c)

Figure 9: $\mathrm{FI}(Si_2C_3 - \mathrm{III}[a,1])$, $\mathrm{FI}(Si_2C_3 - \mathrm{III}[a,b])$, and $\mathrm{FI}(Si_2C_3 - \mathrm{III}[1,b])$, respectively.

Proof. When $b = 1$, then the graph of $Si_2C_3 - \mathrm{III}[a,1]$ consists of four types of faces, three internal faces f_{14}, f_{20}, and f_{22} and an external face f_∞ having the sum of degrees $20a$. Moreover, the values of $|f_{14}|$, $|f_{20}|$, and $|f_{22}|$ are $2(a-1)$, 2, and $(a-2)$, respectively. The rest follows from the definition of the face index. Now, when $b > 1$, then we notice that the structure $SiC_3 - \mathrm{III}[a,b]$ contains eight types of internal faces, which are f_{14}, f_{15}, f_{17}, f_{18}, f_{21}, f_{22}, f_{23}, and f_{24} and an external face, f_∞. Moreover, the sum of vertex degrees of external face is $20a + 24(b-1)$. In each row of Table 4, the number of internal faces is written. □

Remark 4. It is interesting to observe that $|V(Si_2C_3 - \mathrm{III}[a,b])| = 10ab$, $|E(Si_2C_3 - \mathrm{III}[a,b])| = 15ab - 2a - 3b$, and $|F(Si_2C_3 - \mathrm{III}[a,b])| = 5ab - 32 - 3b + 2$. Hence, the structure $Si_2C_3 - \mathrm{III}[a,b]$ satisfies the Euler formula.

With the same settings as in Section 2.1, we present the results obtained for $Si_2C_3 - \mathrm{III}[a,b]$ in a graphical way in Figure 9.

3. Conclusions

An ongoing direction in mathematical and computational chemistry is the assessment of various properties of molecular structures with the help of numerical graph descriptors. These invariants have also established the feasible applications in QSAR/QSPR studies, which are beneficial for the new molecular designs, drug discoveries, and hazard estimation of chemicals. Hence, the novel index, named as the face index for the molecular graphs of silicon carbides, is presented through the numerical way, and we have also displayed our numeric outcomes in the graphical way. Our consequences could be applicable in assessing and comparing the properties of these molecular structures.

Data Availability

The data used to support the findings of the study are included within the article.

Conflicts of Interest

The authors declare no conflicts of interest.

Acknowledgments

This work was supported in part by the National Key Research and Development Program under Grants 2017YFB0802300 and 2018YFB0904205 and Key Laboratory of Pattern Recognition and Intelligent Information Processing, Institutions of Higher Education of Sichuan Province under Grant MSSB-2020-12.

References

[1] L. Luo, N. Dehgardi, and A. Fahad, "Lower bounds on the entire Zagreb indices of trees," *Discrete Dynamics in Nature and Society*, vol. 2020, Article ID 8616725, 8 pages, 2020.

[2] Z. Shao, P. Wu, Y. Gao, I. Gutman, and X. Zhang, "On the maximum ABC index of graphs without pendent vertices," *Applied Mathematics and Computation*, vol. 315, no. 315, pp. 298–312, 2017.

[3] Z. Shao, P. Wu, H. Jiang, S. M. Sheikholeslami, and S. Wang, "On the maximum ABC index of bipartite graphs without pendent vertices," *Open Chemistry*, vol. 18, no. 1, pp. 39–49, 2020.

[4] Z. Shao, P. Wu, X. Zhang, D. Dimitrov, and J.-B. Liu, "On the maximum ABC index of graphs with prescribed size and without pendent vertices," *IEEE Access*, vol. 6, no. 6, pp. 27604–27616, 2018.

[5] S. Wang, C. Wang, L. Chen, J. B. Liu, and Z. Shao, "Maximizing and Minimizing Multiplicative Zagreb Indices of graphs subject to given number of cut edges," *Mathematics*, vol. 6, pp. 1–10, 2018.

[6] W. Gao, W. Wang, and M. R. Farahani, "Topological indices study of molecular structure in anticancer drugs," *Journal of Chemistry*, vol. 2016, Article ID 3216327, 8 pages, 2016.

[7] A. Ye, M. I. Qureshi, A. Fahad et al., "Zagreb connection number index of nanotubes and regular hexagonal lattice," *Open Chemistry*, vol. 17, no. 1, pp. 75–80, 2019.

[8] D. Zhao, Z. Iqbal, R. Irfan et al., "Comparison of irregularity indices of several dendrimers structures," *Processes*, vol. 7, no. 10, p. 662, 2019.

[9] J. Zheng, Z. Iqbal, A. Fahad et al., "Some eccentricity-based topological indices and polynomials of oly (EThyl-eneAmidoAmine) (PETAA) dendrimers, processes," vol. 7, no. 433, pp. 1–14, 2019.

[10] X. Zuo, J.-B. Liu, H. Iqbal, K. Ali, and S. T. R. Rizvi, "Topological indices of certain transformed chemical structures," *Journal of Chemistry*, vol. 2020, Article ID 3045646, 7 pages, 2020.

[11] J.-B. Liu, M. Javaid, and H. M. Awais, "Computing zagreb indices of the subdivision-related generalized operations of graphs," *IEEE Access*, vol. 7, pp. 105479–105488, 2019.

[12] J.-B. Liu, J. Zhao, S. Wang, M. Javaid, and J. Cao, "On the topological properties of the certain neural networks," *Journal of Artificial Intelligence and Soft Computing Research*, vol. 8, no. 4, pp. 257–268, 2018.

[13] W. F. Wang and W. Gao, "Second atom-bond connectivity index of special chemical molecular structures," *Journal of Chemistry*, vol. 2014, Article ID 906254, 8 pages, 2014.

[14] A. R. Katritzky, R. Jain, A. Lomaka, R. Petrukhin, U. Maran, and M. Karelson, "Perspective on the relationship between melting points and chemical structure," *Crystal Growth & Design*, vol. 1, no. 4, pp. 261–265, 2001.

[15] H. Wiener, "Structural determination of paraffin boiling points," *Journal of the American Chemical Society*, vol. 69, no. 1, pp. 17–20, 1947.

[16] J. A. Bondy and U. S. R. Murty, *Graph Theory*, Springer, Berlin, Germany, 2008.

[17] M. K. Jamil, M. Imran, and K. Abdul Sattar, "Novel face index for benzenoid hydrocarbons," *Mathematics*, vol. 8, no. 3, p. 312, 2020.

[18] A. Norlin, J. Pan, and C. Leygraf, "Investigation of interfacial capacitance of Pt, Ti and TiN coated electrodes by electrochemical impedance spectroscopy," *Biomolecular Engineering*, vol. 19, no. 2-6, pp. 67–71, 2002.

[19] S. Singh and R. C. Buchanan, "SiC-C fiber electrode for biological sensing," *Materials Science and Engineering: C*, vol. 27, no. 3, pp. 551–557, 2007.

[20] R. Gerhardt, *Properties and Applications of Silicon Carbide*, BoDBooks on Demand, Norderstedt, Germany, 2011.

[21] G. L. Harris, *Properties of Silicon Carbide*, IET, London, UK, 1995.

[22] H. J. Kang, J. H. Moon, W. Bahng et al., "Oxygen- and photoresist-related interface states of 4H-SiC Schottky diode observed by deep-level transient spectroscopy," *Journal of Applied Physics*, vol. 122, no. 9, Article ID 094504, 2017.

[23] S. M. Koo, *Design and process issues of junction-and ferroelectric-field effect transistors in silicon carbide*, Ph.D. thesis, Doctoral dissertation, Mikroelektronik och informationsteknik, KTH Royal Institute of Technology, Stockholm, Sweden, 2003.

[24] Z.-Q. Cai, A. Rauf, M. Ishtiaq, and M. K. Siddiqui, "On ve-degree and ev-degree based topological properties of silicon carbide Si2C3-II [p, q]," *Polycyclic Aromatic Compounds*, pp. 1–15, 2020.

[25] W. Gao and W. F. Wang, "The fifth geometric-arithmetic index of bridge graph and carbon nanocones," *Journal of Difference Equations and Applications*, vol. 23, no. 1-2, pp. 100–109, 2017.

[26] X.-L. Wang, J.-B. Liu, A. Jahanbani, M. K. Siddiqui, N. J. Rad, and R. Hasni, "On generalized topological indices of silicon-carbon," *Journal of Mathematics*, vol. 2020, Article ID 2128594, 21 pages, 2020.